An MRI study of the corpus callosum in monkeys: Developmental trajectories and effects of neonatal hippocampal and amygdala lesions

Christa Payne, *Emory University*
Laetitia Cirilli, *Emory University*
Jocelyne Bachevalier, *Emory University*

Final published version: http://dx.doi.org/10.1002/dev.21514

Copyright information:

A MRI STUDY OF THE CORPUS CALLOSUM IN MONKEYS: DEVELOPMENTAL TRAJECTORIES AND EFFECTS OF NEONATAL HIPPOCAMPAL AND AMYGDALA LESIONS

Christa Payne, **Laetitia Cirilli**, and **Jocelyne Bachevalier**

Yerkes National Primate Research Center, Emory University, Atlanta, GA, 30329

Abstract

This study provides the first characterization of early developmental trajectories of corpus callosum (CC) segments in rhesus macaques using noninvasive MRI techniques and assesses long-term effects of neonatal amygdala or hippocampal lesions on CC morphometry. In Experiment 1, ten monkeys (5 males) were scanned at 1 week – 2 years of age; eight additional infants (4 males) were scanned once at 1 – 4 weeks of age. The first 8 months showed marked growth across all segments, with sustained, albeit slower, growth through 24 months. Males and females had comparable patterns of CC maturation overall, but exhibited slight differences in the anterior and posterior segments, with greater increases in the isthmus for males and greater increases in the rostrum for females. The developmental changes are likely a consequence of varying degrees of axonal myelination, redirection, and pruning. In Experiment 2, animals with neonatal lesions of the amygdala (n=6; 3 males) or hippocampus (n=6; 4 males) were scanned at 1.5 years post-surgery and compared to scans of six control animals from Experiment 1. Whereas amygdala damage yielded larger rostral and posterior body segments, hippocampal damage yielded larger rostrum and isthmus. These differences demonstrate that early perturbations to one medial temporal lobe structure may produce extensive and long-lasting repercussions in other brain areas. The current findings emphasize the complexity of neural circuitry putatively subserving neurodevelopmental disorders such as autism spectrum disorder and Williams syndrome, which are each characterized by malformations and dysfunction of complex neural networks that include regions of the medial temporal lobe.

Keywords

commissure; *Macaca mulatta*; neurodevelopment; neuroimaging; nonhuman primate; rhesus macaque; structural; volumetric

---

The corpus callosum (CC) is the major commissural fascicle of the brain and provides a rapid topographic transfer of information between homologous areas of the left and right

Corresponding Author: Christa Payne, 1920 Briarcliff Road NE/Atlanta, Georgia 30062, office: 404.785.8426, fax: 404.785.9063, christa.payne@emory.edu.

Christa Payne is now at Marcus Autism Center, Children's Healthcare of Atlanta, Emory School of Medicine, Department of Pediatrics, Division of Autism and Related Disabilities, Atlanta, GA, 30329. Laetitia Cirilli is now at DSM Food Specialties, La Ferté sous Jouarre, France.

hemispheres. It is the major commissure for the interhemispheric connectivity, and can be segmented into distinct regions based on the fibers of origin (Schmahmann & Pandya, 2006; Witelson, 1989), giving the commissure a functional topography. The CC has also been implicated in several aspects of cognitive functioning. It integrates the activities of the two hemispheres by unifying sensory information (Berlucchi, Aglioti, Marzi, & Tassinari, 1995; Shanks, Rockel, & Powel, 1975), controlling bimanual motor actions (Eliassen, Baynes, & Gazzaniga, 2000; Schlaug, Jancke, Huang, Staiger, & Steinmetz, 1995; Zaidel & Sperry, 1977), and regulating higher-order cognitive abilities (Cook, 1984; Levy & Trevarthen, 1981; Takeuchi et al., 2010; Zahr, Rohlfing, Pfefferabaum, & Sullivan, 2009; Zaidel & Sperry, 1974).

Histological investigations of post-mortem tissue have provided insight into the organization and cellular development of the CC in humans and nonhuman primates (LaMantia & Rakic, 1990a, 1990b; Rakic & Yakovlev, 1968). Given that most of the functions supported by the CC undergo significant changes from birth to adolescence, effort has been made in the last two decades to trace the normative development of the CC in humans as well as in several nonhuman primate species, using longitudinal design with noninvasive structural MRI and density tensor imaging (DTI) techniques. In humans, sharp increases in midsagittal area of the CC have been reported between 5–18 years, and particularly in its most posterior segment, the splenium (Giedd et al., 1996, 1999; Luders, Thompson, & Toga, 2010). A similar developmental course was recently reported in chimpanzees between 6–54 years (*Pan troglodytes*) (Hopkins & Phillips, 2010), baboons (*Papio Hamadryas*) from prenatal age to postnatal week 32 (Phillips & Kochunov, 2011), bonnet macaques (*Macaca radiata*) from juvenile age to adults (Pierre, Hopkins, Taglialatela, Lees, & Bennett, 2008), and capuchin monkeys (*Cebus paella*) from 4 days to 20 years (Phillips & Sherwood, 2012). In rhesus monkeys (*Macaca mulatta*), Franklin and colleagues (2000) used structural MR images to measure the total surface of the CC on the midsagittal axis as well as the area of the splenium in male and female rhesus monkeys from 8 months to 7.2 years of age. They reported a steady increase in CC surface area until 4.5 years, with males having 20% larger CC than females, mostly in the splenium subregion. More recently, Knickmeyer and colleagues (2010) traced brain development in rhesus monkeys from 10 to 64 months of age and reported a steady increase in CC volume within this age range that parallels steady changes in DTI properties in the genu and splenium during this period (Shi et al., 2013).

None of these studies, however, investigated the developmental trajectory of the CC in early infancy in monkeys. Given the early manifestation of disorders such as autism spectrum disorder (ASD) and Williams Syndrome (WS) and the challenges associated with studying brain development during this early developmental period in humans, characterizing early brain development in rhesus monkeys is an important component of advancing our understanding of neural malformation and dysfunction associated with human neurodevelopmental disorders. Thus, to fill this gap of knowledge, the first aim of the present study investigated the developmental trajectory of the CC in rhesus monkeys from birth to age 2 years, using structural MR imaging.

The development of the CC has also been shown to be sensitive to early brain insult and changes in surface area and white matter integrity have been associated with several

developmental disorders in humans, such as ASD (Aoki, Abe, Nippashi, & Yamasue, 2013; Frazier & Hardan, 2009; Freitag et al., 2009; Travers et al., 2012) and WS (Luders et al., 2007). These neurodevelopmental disorders have been consistently associated with behavioral abnormalities, increased stress and anxiety, and impairments in social communication and cognitive functions (Brock, Brown, & Boucher, 2006; Sampaio, Sousa, Férnandez, Henriques, & Gonçalves, 2008; Vicari, Brizzolara, Carlesimo, Pezzini, & Volterra, 1996; Volkmar, Lord, Bailey, Schultz, & Klin, 2004) as well as dysfunction of the limbic structures, such as the amygdala and/or the hippocampus (Allely, Gillberg, & Wilson, 2014; Bauman & Kemper, 1985, 2005; Capitão et al., 2011; Haas et al., 2014; Meda, Pryweller, & Thornton-Wells, 2012; Raymond, Bauman, & Kemper, 1996; Saitoh, Karns, & Courchesne, 2001). The impact that limbic dysfunction has on other brain regions has not yet been fully elucidated. An essential step in understanding the effect of early limbic dysfunction on the integrity of different neural networks is to characterize morphological changes associated with early limbic disturbances. Although neither the amygdala nor the hippocampus send interhemsipheric projections directly via the CC, both structures are heavily connected with cortical regions that have dense interhemispheric connectivity via the CC, such as the prefrontal, cingulate, parietal and temporal cortices. Characterizing the effect of early limbic disruption on CC size may help elucidate the relationship between CC disruption and developmental disruptions of the limbic system. Thus, the second aim of this study was to investigate volumetric changes of the CC in juvenile monkeys that had received lesions of the amygdala and hippocampus in the first week of life. Preliminary reports of the findings were published in abstract form (Cirilli, Payne & Bachevalier, 2009; Payne, Machado, Jackson, & Bachevalier, 2005).

MATERIALS AND METHODS

All procedures were approved by the Animal Care and Use Committee of the University of Texas Health Science Center, Houston and carried out in accordance with the National Institutes of Health Guide for the care and Use of Laboratory Animals. Every effort was made to minimize the number of animals used, as well as any pain and suffering.

Subjects

A total of twenty-six rhesus monkeys (*Macaca mulatta*; thirteen male) were used in this study (nineteen Experiment 1 and eighteen in Experiment 2; see below). All monkeys were born at the Keeling Center for Comparative Medicine and Research in Bastrop, Texas and surrogate-peer reared at the University of Texas Health Science Center in Houston, Texas in a socially enriched nursery environment to promote species-specific socioemotional skills (Burbacher et al., 2013; Goursaud & Bachevalier, 2007; Rommeck, Capitanio, Strand, & McCowan, 2011). The animals also served as control subjects for multiple experiments of memory, emotional reactivity, social behavior and reward assessment that occurred concurrently with the present study and thus received extensive cognitive enrichment.

Surrogate Peer-rearing Conditions

A principal human caregiver provided care of infants 6 hours a day, 5 days a week. During weekends, familiar human caregivers fed, handled and played with the infants 2–4 h a day.

Infants were individually housed in size-appropriate wire cages under open radiant incubators that allowed physical contact with animals in neighboring cage(s), and visual, auditory, and olfactory contact with all other infants in the nursery. Each infant was provided a synthetic plush surrogate (30cm in length) and cotton towels for contact comfort. Infants interacted multiple times a day with age-matched peers while their home cages were cleaned and the plush surrogates and cotton towels were changed. Beginning at 1 month of age, which allowed for sufficient healing from surgery, infants socialized daily with three other age- and sex-matched peers in a large play cage, containing toys and towels, located in the primate nursery (3–4h, 5 days/week). At 3 months of age, infants were transferred to larger cages and individually housed with a large central mesh separating two adjacent cages that allowed visual and physical contact possible between pairs of infants. They were socialized in a large enclosure with three other matched peers containing toys and blankets. At 7 months of age, monkeys were housed in quads in large enclosures and beginning at 12 months, they were housed in pairs. During this first year, monkeys were also trained in several memory tasks and tested for emotional reactivity. Our surrogate-peer rearing is analogous to the 'continuous rotation peer rearing' condition known to produce a biobehavioral profile that is most comparable to those of mother-reared monkeys (Rommeck et al., 2011).

Experiment 1: Development of CC

Subjects

Nine male and ten female rhesus monkeys (*Macaca mulatta*) were used in this experiment. Ten animals (five male) received multiple imaging sessions (range: 2–9 scans) between 1 week and 2 years of age. Five of these animals received sham-operations (described below in Experiment 2) and five were unoperated controls. An additional unoperated control (female) was scanned once at 7.5 months of age. Eight monkeys (four male) were scanned once within the first month of life (of these, five (three male) received neonatal neurotoxic lesions of the amygdala or hippocampus; described below in Experiment 2). A total of 66 scans (30 scans of nine males; 36 scans of ten females) were used to assess CC growth.

MRI Acquisition

A full description of the scanning procedures is available in our assessment of the volumetric maturation of the total cerebrum, amygdala and hippocampus in these animals (Payne, Machado, Bliwise, & Bachevalier, 2010); therefore only a brief account is provided here. Animals between 1 week and 8 months old were removed from their cage and sedated with isoflurane (1–2% to effect) in an induction box. Animals older than 8 months were immobilized with ketamine hydrochloride (10mg/kg) prior to transport from home cage. All animals were intubated to allow for isoflurane anesthesia during the scan, brought to the MRI facility, and placed in a nonferrous stereotaxic apparatus (Crist Instruments Co., Inc., Damascus, MD). Scans were acquired in a GE Signa 1.5 Tesla Echo Speed scanner (GE Medical Systems, Milwaukee, WI) using a circular surface coil (3" for animals less than 1 month, 5" for animals greater than 1 month). A 2D high resolution T1-weighted imaging spin-echo sequence (TR = 450 msec, TE = 11 msec, FOV = 12 cm, acquisition matrix = 256 × 192) was obtained in the sagittal plane at 4 mm intervals. The surface area of the CC was

assessed on the midline slice of the sagittal scan and the surface area of the entire midsagittal slice was also measured as an estimate of total cerebral volume.

Surface Area Measurements

Two trained observers used the ImageJ software (v. 1.40; http://rsb.info.nih.gov/ij/) to measure the surface area (SA in mm^2) of the midline brain (including ventricles if present) and surface of the CC (Inter-rater reliability r > 0.90).

Midline surface area boundaries—Midline surface area (SA in mm^2) of the brain included the telencephalon, diencepalon and the midbrain above the superior aspect of the pons (Figure 1A) as well as the ventricle. When the brainstem was visible, the ventral border of the measurement was either the notch superior to the pons or the entry points of the cerebellar peduncles (Figure 1A). No portion of the cerebellum, optic chiasm, brainstem, or midbrain below the superior aspect of the pons was included in the midline total brain SA measurement.

CC boundaries—The midsagittal image was used to trace the CC boundaries. Following the segmentation paradigm described by Witelson (1989) and used by Giedd and colleagues (1996, 1999), the CC was segmented into seven subregions (rostrum, genu, rostral body, anterior midbody, posterior midbody, isthmus, and splenium; Figure 1B and 1C). Surface area was recorded for each segment and summed to obtain the total CC area.

Data Analysis

SPSS$^©$ Statistics software was used for all statistical analyses (v.21; IBM Corp.). Hierarchical linear mixed-effects modeling was used to characterize the influence of age and sex on the development of the CC and brain size (as estimated by the midline surface area (MSA)). This procedure accounts for irregular intervals between measurements, correlated within-subject variance and unequal variances. Pearson's r correlation analysis between measured MSA and previously assessed Total Cerebral Volume (Payne et al., 2010) was used to confirm that MSA was an appropriate estimate of brain size (r = 0.923, $p < 0.0001$). Linear and curvilinear (quadratic, cubic and power) patterns were first modeled with Age, Sex and MSA (centered separately for males and females to reduce nonessential colinearity). F-tests and log-likelihood ratios were used to determine whether a linear, quadratic, cubic, or power relationship best described the data. All trajectories were modeled including the MSA in order to represent the unique growth of each region.

Results

A scatterplot representing the raw data for the CC surface area is illustrated in Figure 2, and modeled developmental trajectories are presented in Figure 3. Multiple functions adequately characterized the growth trajectories for all the regions assessed; however, the power function provided the best characterization of the data in each case, and therefore is the only function represented graphically and described below.

For the CC as a whole, there was a significant effect of Age (F(1,52.784) = 153.280, $p < 0.0001$) that was best explained by the function $y = 31.745x^{0.1633}$ (Figure 3A). Total CC

surface area increased substantially (113.53%) between one week and two years of age and is characterized by a period of rapid growth until approximately 7.5 months of age, at which point the rate of growth begins to level off (Figure 3B).

Significant effects of Age were also observed between one week and two years of age separately for the rostrum ($F(1,28.704) = 13.141$, $p = 0.001$; 73.41% increase), genu ($F(1,49.406) = 38.450$, $p < 0.0001$; 82.12% increase), rostral body ($F(1,19.149) = 41.884$, $p < 0.0001$; 81.03% increase), anterior midbody ($F(1,58.530) = 48.263$, $p < 0.0001$; 80.96% increase), posterior midbody ($F(1,64.916) = 115.642$, $p < 0.0001$; 92.16% increase), isthmus ($F(1,57.670) = 128.147$, $p < 0.0001$; 73.90% increase), and splenium ($F(1,56.352) = 272.338$, $p < 0.0001$; 106.03% increase). Figure 3C illustrates the power function modeled across all cases for the rostrum ($y = 2.0847x^{0.1185}$), genu ($y = 8.2092x^{0.1291}$), rostral body ($y = 5.7264x^{0.1278}$), anterior midbody ($y = 3.6888x^{0.1277}$), posterior midbody ($y = 3.2026x^{0.1406}$), isthmus ($y = 2.8097x^{0.1191}$) and splenium ($y = 7.9345x^{0.1556}$). As in the CC overall, each segment was characterized by a period of rapid growth until 7–8 months of age, followed by subtle yet sustained growth into the second year of life (Figure 3D).

Sex differences were noted in two segments: a trend for an Age × Sex interaction in the rostrum ($F(1,13.974) = 4.286$, $p = 0.057$), and a significant Age × Sex interaction in the isthmus ($F(1,46.551) = 7.579$, $p = 0.008$). In the rostrum, females exhibited more robust effects of Age than males (males: $F(1,13.410) = 3.398$, $p = 0.087$; 36.71% increase; females: $F(1,34.971) = 10.583$, $p = 0.003$; 68.69% increase), and females had a larger rostrum throughout the developmental period. Figure 3E illustrates the power functions of rostrum growth modeled separately for males ($y = 2.0382x^{0.0673}$) and females ($y = 2.1357x^{0.1126}$). In the isthmus, both sexes exhibit robust effects of Age (males: $F(1,23.772) = 160.665$, $p < 0.0001$; 157.43% increase; females: $F(1,33.160) = 31.226$, $p < 0.0001$; 67.66% increase). Figure 3F illustrates the power functions of isthmus growth modeled separately for males ($y = 2.5975x^{0.2036}$) and females ($y = 2.9852 \times^{0.1113}$).

Experiment 2: Effect of Early Amygdala or Hippocampal Lesion on CC Size

Subjects

Eighteen juvenile rhesus monkeys (14–18.5 months of age) were used in this portion of the project. Eleven of the monkeys scanned during the first 2 weeks as part of Experiment 1 and one additional monkey subsequently received neurotoxic lesions of either the amygdala (NEO-A$_{ibo}$; n=6; three males) at 7–17 days of age or the hippocampus (NEO-H$_{ibo}$; n=6; four males) at 7–25 days of age. Scans from a subset of six control animals from the developmental analyses in Experiment 1 (three males) matched for age of scan were used for comparison. The animals in this comparison control group (CONT) either received sham operations at 8–10 days of age (n=3; one male) or were un-operated controls (n=3; two males).

MRI-guided surgery

A full description of all surgical techniques has been published in previous reports (Goursaud & Bachevalier, 2007; Kazama, Heuer, Davis, & Bachevalier, 2012; Zeamer,

Heuer, & Bachevalier, 2010). Briefly, a T1-weighted FSPGR-echo sequence scan (T1 = 600 msec, TR = 2500 msec, TE = 25 msec, FOV = 12 cm with number of excitations (NEX) = 2, acquisition matrix = 256×256) in the coronal plane at 1mm intervals was used to calculate neurotoxin injection coordinates; and a Fluid Attenuated Inversion Recovery (FLAIR) protocol (TE = 140 msec, TR = 10000 msec, inversion time (TI) = 2200, contiguous 3 mm sections, 12 cm FOV, 256×256 matrix) was acquired to select the injection sites pre-surgically and facilitate the estimation of lesion extent post-surgery. All surgical procedures were performed under deep anesthesia (ketamine hydrochloride, 10mg/kg, i.m., followed by isoflurane gas, 1.0– 2.0%, v/v, to effect) using aseptic techniques. The scalp and connective tissue were incised and gently retracted together. Small bilateral craniotomies were created above the injection sites and slits were cut in the dura bilaterally to allow 10ml Hamilton syringes filled with ibotenic acid (Biosearch Technologies, Novato, CA, 10mg/ml in phosphate buffered saline, pH 7.4) to be lowered to the appropriate injection coordinates within the amygdala or hippocampus bilaterally. For sham lesions, bilateral craniotomies similar to those used for lesions were made and the dura was cut bilaterally, but no needle penetrations occurred. All animals received pre- and post-surgical treatments to minimize risk of infection (Cephazolin, 25mg/kg, p.o.), control swelling (dexamethazone sodium phosphate, 0.4mg/kg, s.c.), and relieve pain (acetaminophen, 10mg/kg, p.o.).

MRI Measurements

Previous reports on these animals (Goursaud & Bachevalier, 2007; Zeamer et al., 2010) have fully characterized the extent of damage estimated from FLAIR images acquired one week after surgery that allow for the visualization of the edema associated with cell death following ibotenic acid lesions. These reports showed that the lesions were largely as intended with minimal unintended damage. Since group comparisons in this study were completed on scans acquired approximately one year after surgery, the percent of volume reduction was calculated using the T1-weighted coronal sequence acquired in the same scanning session. A rater blind to experimental group measured the CC surface area using the procedure described above in Experiment 1 and the volumes of the amygdala and hippocampus with ImageJ software (http://rsb.info.nih.gov/ij/) using our previously reported procedure (Payne et al., 2010). Briefly, bilateral surface area measurements were taken on each image throughout the extent of the structure. The measured surface area of each section was summed and multiplied by image thickness to calculate a total volume of damage (Gundersen & Jensen, 1987). The percent reduction for each case was then calculated using the following formula: [100 – volume/average control volume]*100.

Data Analysis

Group differences were analyzed separately (CONT vs. NEO-A_{ibo} or CONT vs. NEO-H_{ibo}) for the Total CC and the seven individual segments, correcting for overall brain size (as estimated by the MSA). Because previous studies indicate that males and females may exhibit differences in brain size, as well as the sex differences noted in Experiment 1, sex was included as a factor in the comparisons between group CONT and group NEO-A_{ibo}. Sex was not balanced across group NEO-H_{ibo} (four males, two females), therefore sex differences were not assessed in the comparisons between group CONT and group NEO-H_{ibo}. Differences in Total CC area were assessed using a 2×2 ANCOVA with Group (CONT

and NEO-A$_{ibo}$ or NEO-H$_{ibo}$) and Sex (male, female) as between-subjects factors and midline surface area as a covariate. Differences across individual segments of the CC were assessed using 2×2 MANCOVAs, with planned comparisons. Partial Correlation tests were used to assess the relationship between extent of lesion and CC surface area, controlling for overall brain size.

Results

Volume Reduction Assessment

Table 1 provides a summary of the volume reduction across all cases. The average combined amygdala volume reduction observed within group NEO-A$_{ibo}$ was 31.0%, and the average combined hippocampal volume reduction observed within group NEO-H$_{ibo}$ was 42.3%.

Effects of lesions on Total CC

Effect of Neonatal Amygdala Damage—Groups NEO-A$_{ibo}$ and CONT did not differ in total CC surface area (F(1,7) = 0.573, p = 0.474; η_p^2 = 0.076; Figure 4A) and males and females did not differ (F(1,7) = 1.422, p = 0.272; η_p^2 = 0.169). There were no correlations between total CC surface area and amygdala volume.

Effect of Neonatal Hippocampal Damage—CC total surface area was slightly smaller in group NEO-H$_{ibo}$ as compared to group CONT (Figure 4A), but this reduction did not reach significance (F(1,9) = 0.104, p = 0.755; η_p^2 = 0.011). However, there was a tendency for a negative relationship between CC surface area and the volume reduction of the left hippocampus (r$_p$(3) = −0.864, p = 0.059; Figure 4B), indicating greater reduction in CC surface area in animals with more extended hippocampal damage.

Effects of lesions on CC Segments

Effect of Neonatal Amygdala Damage—Group differences were observed when the surface area of the individual CC segments was analyzed (see Table 2). Specifically, compared to group CONT, group NEO-A$_{ibo}$ had a larger rostral body (F(1,7) = 7.553, p = 0.029; η_p^2 = 0.519; Figure 5B) and posterior midbody (F(1,7) = 6.057, p = 0.043; η_p^2 = 0.464; Figure 5C). There were no significant sex differences at any segment.

Effect of Neonatal Hippocampal Damage—Compared to group CONT, group NEO-H$_{ibo}$ had a larger rostrum (F(1,9) = 6.021, p = 0.037; η_p^2 = 0.401; Figure 5A) and a tendency for a larger isthmus (F(1,9) = 3.983, p = 0.077; η_p^2 = 0.307; Figure 5D). Sex differences were not assessed in this group.

DISCUSSION

These experiments demonstrate that early maturation of the rhesus CC is detectable with structural MRI and shows marked increases in all CC segments throughout the first 8 months with sustained, yet reduced, growth thereafter through 24 months. Additionally, neonatal lesions of either the amygdala or hippocampus result in notable areal changes in the CC at approximately 15.5 months, specifically in the anterior and posterior segments.

Developmental trajectory of the CC

Our results further the current understanding of CC maturation in rhesus macaques using structural MRI. Franklin and colleagues (2000) reported a positive correlation between CC size and age between one and five years. Knickmeyer and colleagues (2010) demonstrated linear growth in CC white matter between 10 and 64 months. Unlike these previous reports, our study captures the early maturation of the CC beginning at one week of age. The inclusion of these earliest time points drives the identification of the rapid development until around eight months (younger than the earliest age in previous studies) followed by an extended period of slower, yet sustained, growth (corresponding to the development observed in previous studies). Our data parallel earlier electron microscopic analyses during fetal and early postnatal ages (LaMantia & Rakic, 1990) that demonstrated an overproduction of CC axons at birth that are then eliminated during the first postnatal months.

Our study is the first description of developmental trajectories for the CC regions in rhesus macaques. The individual CC segments exhibited similar patterns as the total CC and parallel the changes reported in humans (Luders et al., 2010). Although MRI cannot parse out the contributions of biological mechanisms on the CC size, variation in CC size is likely the consequence of varying degrees of axonal myelination, redirection, and pruning. Males and females had comparable maturation across most segments, but showed slight differences in the rostrum and isthmus, such that females showed more robust areal increases in the rostrum and males showed more robust increases in the isthmus. Although sex differences have not previously been reported and need to be verified in a larger cohort, the observed differences align with observations of maturational sex differences in abilities associated with the prefrontal cortex (main fibers of passage through the rostrum) (Unterrainer et al., 2013) and the parietal and temporal cortices (main fibers of passage through the isthmus) (Rosselli, Ardila, Maute, & Inozemtseva, 2009).

Effects of neonatal amygdala and hippocampal lesions

The results of the second experiment highlight the relationship between the CC and limbic areas. Although there were no differences in the size of the total CC across groups, early damage to either the amygdala or hippocampus had long-lasting effects on the size of unique segments of CC that represent functional and structural domains. Previous work has shown that including measurements from additional slices adjacent to the midsagittal slice can increase the ability to detect group difference in the CC (Wade et al., 2013). Although the current study minimized movement and standardized the angle of the midsagittal slice with sedation and stabilizing and centering the animals' heads in a stereotaxic apparatus, the inclusion of additional slices should be used in future investigations. The current data demonstrate subtle differences in CC areal abnormalities following neonatal lesions of the amygdala or hippocampus, and are consistent with findings that prenatal stress, which alters the development of the limbic structures, results in altered CC size in rhesus macaques (Coe, Lulbach, & Schneider, 2002; Howell, et al., 2013). This suggests that focal damage to one structure participating in an intricate neural network may have widespread and long lasting repercussions in other areas.

Whereas total CC surface area in animals with neonatal amygdala lesions was in the normal range, analyses of separate CC segments revealed moderate but significant increases of the rostral body and the posterior midbody. Although the amygdala does not directly project to the motor or premotor cortices, it has strong interconnections with the cingulate motor cortex, both its anterior (M3) and mid-posterior (M4) regions (Gothard, 2014; Morecraft et al., 2007; Paus, 2001). In turn, these cingulate motor areas innervate the frontal motor and premotor cortex. Thus, neonatal amygdala lesions may have impacted the normal development of the cingulate motor cortex, which in turn resulted in abnormal maturation of the motor and premotor interhemispheric projections through the rostral body and posterior midbody CC subregions.

Neonatal hippocampal lesions altered different CC segments. Although the total CC surface area in animals with neonatal hippocampal lesions did not differ from control animals, there was a significant negative correlation between the size of the total CC and the percent reduction in hippocampal volume, indicating that more substantial hippocampal damage was associated with smaller CC. Despite this association, reliable increases were observed in the rostrum and the isthmus of animals with early hippocampal damage, indicating a differential effect of hippocampal damage across CC segments. The observed increases in the rostrum and isthmus following neonatal hippocampal lesions are likely a result of dysregulated maturational processes between the hippocampus (via the fornix) and/or the entorhinal cortex (via the uncinate fascicle) with the ventromedial prefrontal cortex and retrosplenial regions (Cavada, Compañy, Tejedor, Cruz-Rizzolo, & Reinoso-Suárez, 2000; Croxson et al., 2005; Insausti & Amaral, 2008; Lavenex, Suzuki & Amaral, 2002; Rosene & Van Hoesen, 1977; Ungerleider, Gaffan, & Pelak, 1989), which send interhemispheric projections through rostrum and isthmus subregions of the CC, respectively (Schmahmann & Pandya, 2006; Witelson, 1989).

It is interesting to note that both types of neonatal lesions resulted in increased surface area of specific CC segments. Although the precise processes by which this increase has occurred cannot be determined by the present study, increased CC white matter may have resulted from increased myelination, abnormal axonal redirection and/or decreased pruning of the interhemispheric fibers. Further post-mortem morphological investigations will be needed to determine which of these processes may have accounted for the changes observed.

Alterations in human CC size have been associated with impaired social (Alexander et al., 2007) and cognitive (Alexander et al., 2007; Just, Cherkassky, Keller, Kana, & Minshew, 2007, Just, Cherkasskey, Keller, & Minshew, 2004; Koshino, Kana, Keller, Cherkassky, Minshew, & Just, 2008) functioning, two domains associated with the amygdala and hippocampus. Therefore, it is not surprising that animals with neonatal amygdala lesions and those with neonatal hippocampal lesions showed impairments on functions that have either been attributed to damage to these limbic structures or require coordination between these limbic structures and other brain areas. Notably, the neonatal amygdala lesions yielded significant deficits in functions associated with the amygdala, i.e. emotional reactivity (Raper, Wilson, Sánchez, & Bachevalier, 2011), fear learning (Kazama et al., 2012) and stimulus-reward associations (Kazama & Bachevalier, 2012), as well as in flexible decision-making skills requiring the interactions of the amygdala and the orbital frontal cortex

(Kazama & Bachevalier, 2013). Likewise, the neonatal hippocampal lesions resulted in object and spatial relational memory loss (Alvarado, Kazama, Zeamer, & Bachevalier, 2011; Blue, Kazama & Bachevalier, 2013; Glavis-Bloom, Alvarado, & Bachevalier, 2013; Zeamer & Bachevalier, 2013, Zeamer, Resende, Heuer, & Bachevalier, 2007), as well as impaired working memory processes requiring the interactions between the hippocampus and the lateral prefrontal cortex (Heuer & Bachevalier, 2011, 2013). The observed cognitive deficits in these animals are likely associated not only to direct damage to the limbic structures but also to areal changes in the CC reflecting aberrant interhemispheric connectivity between the prefrontal, premotor, cingulate, parietal and superior temporal cortices. Such interactions may likewise subserve the widespread neural and cognitive changes generally observed in neurodevelopmental disorders, such as ASD and WS (Freitag et al., 2009; Hadjikhani, Joseph, Snyder, & Tager-Flusberg, 2006; Machado & Bachevalier, 2003; Waiter et al., 2005).

Potential impact of rearing conditions

It is important to note that brain maturation is influenced by both genetic factors and environmental conditions, and perturbations in either factor may affect the normal maturation of the brain. The monkeys in this study came from the same genetic pool and had similar experience from birth to adulthood; however, the environment in which they were raised may have impacted the results of this investigation. Previous studies have shown that rearing environment can have profound biobehavioral effects, including MRI measurements of the CC (Sánchez, Hearn, Do, Rilling, & Herndon, 1998). However, there are several reasons to suggest that the effect of our surrogate-peer rearing on the CC changes we observed in this study are not substantial. First, our surrogate-peer rearing environment is analogous to the 'continuous rotation peer rearing' condition described in a systematic investigation of the effects of different nursery rearing styles (Rommeck et al., 2011). This critical investigation found that the type of rearing environment we provided our animals produced a biobehavioral profile most comparable to that of mother-reared monkeys. Second, we previously characterized the developmental trajectory of the hippocampus using the same control animals from Experiment 1 (Payne et al., 2010). The maturational changes we observed in our surrogate-peer reared animals have been replicated in a more recent neuroimaging study using infant monkeys reared with their mothers in large social groups (Hunsaker, Scott, Bauman, Schumann, & Amaral, 2014). The concordance between these two MRI studies suggests that the impact of our surrogate-peer nursery rearing condition on the normal developmental trajectory of the CC (Experiment 1) is unlikely or minimal. These first two points are further substantiated by the observation that the control animals in the present studies developed behavioral and cognitive skills comparable to those found in adult monkeys born and raised in semi-naturalistic environment (Bachevalier, 1990; Blue et al., 2013; Kazama & Bachevalier, 2012, 2013; Zeamer et al., 2007; Zeamer, Kazama, Briseno, & Bachevalier, 2008). Third, we observed differential effects of amygdala and hippocampal lesions on CC segments (Experiment 2). If the changes in surface areas of specific CC segments were a global, unspecific result of our rearing conditions, the affected CC segments should have been similar for both types of lesions. The neonatal amygdala lesions impacted the rostral and mid-posterior body of the CC, whereas the neonatal hippocampal lesions impacted the most posterior segments of the CC. The early insult to the limbic

structures affected the maturation of cortical areas with which they are interconnected, which then altered the development of the interhemispheric connections. Despite the indications that our surrogate-peer rearing environment had minimal impact on our findings, additional systematic investigation is needed to resolve this matter. Future studies will need to replicate the maturational changes and regional differences following neonatal lesions of the limbic structures using a larger number of animals reared in more naturalistic setting.

CONCLUSION

Together the results of the present experiments and previous characterizations of maturational changes in both humans (for review see Lenroot & Giedd, 2006) and rhesus macaques (Franklin et al., 2000; Knickmeyer et al., 2010) further support the use of rhesus monkeys to model human neurodevelopmental disorders, in general, and more specifically, neurodevelopmental disorders characterized by perturbations of the CC. Research is beginning to highlight the importance of considering maturational trajectories when investigating the neural substrates of developmental disorders. Characterizing normal developmental time courses is crucial to elucidating the causes of such disorders, and by extension, identifying biomarkers and developing new interventions for these disorders. Research in nonhuman primates is poised to further our understanding of the synergistic neural relationships that underlie complex human disorders. By demonstrating that neonatal lesions of the amygdala or hippocampus impact CC size long-term, the current study emphasizes the complexity of neural circuitry putatively subserving neurodevelopmental disorders.

Acknowledgments

References

Alexander AL, Lee JE, Lazar M, Boudos R, DuBray MB, Oakes TR, Miller JN, Lu J, Jeong EK, McMahon WM, Bigler ED, Lainhart JE. Diffusion tensor imaging of the corpus callosum in Autism. NeuroImage. 2007; 34(1):61–73. [PubMed: 17023185]

Allely CS, Gillberg C, Wilson P. Neurobiological abnormalities in the first few years of life in individuals later diagnosed with autism spectrum disorder: A review of recent data. Behavioural Neurology. 2014; 2014:210780. [PubMed: 24825948]

Alvarado MC, Kazama A, Zeamer A, Bachevalier J. The effects of selective hippocampal damage on tests of oddity in rhesus macaques. Hippocampus. 2011; 21(10):1137–1146. [PubMed: 20882541]

Aoki Y, Abe O, Nippashi Y, Yamasue H. Comparison of white matter integrity between autism spectrum disorder subjects and typically developing individuals: A meta-analysis of diffusion tensor imaging tractography studies. Molecular Autism. 2013; 4(1):25. [PubMed: 23876131]

Bachevalier J. Ontogenetic development of habit and memory formation in primates. Annals of the New York Academy of Sciences. 1990; 608:457–477. [PubMed: 2127516]

Bauman M, Kemper TL. Histoanatomic observations of the brain in early infantile autism. Neurology. 1985; 35(6):866–874. [PubMed: 4000488]

Bauman M, Kemper TL. Neuroanatomic observations of the brain in autism: A review and future directions. International Journal of Developmental Neuroscience. 2005; 23(2–3):183–187. [PubMed: 15749244]

Berlucchi G, Aglioti S, Marzi CA, Tassinari G. Corpus callosum and simple visuomotor integration. Neuropsychologia. 1995; 33(8):923–936. [PubMed: 8524454]

Blue SN, Kazama AM, Bachevalier J. Development of memory for spatial locations and object/place associations in infant rhesus macaques with and without neonatal hippocampal lesions. Journal of the International Neuropsychological Society. 2013; 19(10):1053–1064. [PubMed: 23880255]

Brock J, Brown GD, Boucher J. Free recall in Williams syndrome: Is there a dissociation between short- and long-term memory? Cortex. 2006; 42(3):366–375. [PubMed: 16771042]

Burbacher TM, Grant KS, Worlein J, Ha J, Curnow E, Juul S, Sackett GP. Four decades of leading-edge research in the reproductive and developmental sciences: The Infant Primate Research Laboratory at the University of Washington National Primate Research Center. American Journal of Primatology. 2013; 75(11):1063–1083. [PubMed: 23873400]

Capitão L, Sampaio A, Sampaio C, Vasconcelos C, Férnandez M, Garayzábal E, Shenton ME, Gonçalves OF. MRI amygdala volume in Williams Syndrome. Research in Developmental Disabilities. 2011; 32(6):2767–2772. [PubMed: 21752593]

Cavada C, Compañy T, Tejedor J, Cruz-Rizzolo RJ, Reinoso-Suárez F. The anatomical connections of the macaque monkey orbitofrontal cortex. A review. Cerebral Cortex. 2000; 10(3):220–242. [PubMed: 10731218]

Cirilli, L., Payne, C., Bachevalier, J. Neuroscience Meeting Planner. Chicago, IL: Society for Neuroscience Online; 2009. Neonatal hippocampal and amygdala lesions alter the development of the corpus callosum: A volumetric MRI study in adult monkeys. Program No. 536.20

Coe CL, Lulbach GR, Schneider ML. Prenatal disturbance alters the size of the corpus callosum in young monkeys. Developmental Psychobiology. 2002; 41(2):178–185. [PubMed: 12209659]

Cook ND. Callosal inhibition: The key to the brain code. Systems Research and Behavioral Science. 1984; 29(2):98–110.

Croxson PL, Johansen-Berg H, Behrens TE, Robson MD, Pinsk MA, Gross CG, Richter W, Richter MC, Kastner S, Rushworth MF. Quantitative investigation of connections of the prefrontal cortex in the human and macaque using probabilistic diffusion tractography. Journal of Neuroscience. 2005; 25:8854–8866. [PubMed: 16192375]

Eliassen JC, Baynes K, Gazzaniga MS. Anterior and posterior callosal contributions to simultaneous bimanual movements of the hands and fingers. Brain: A Journal of Neurology. 2000; 123(pt12): 2501–2511. [PubMed: 11099451]

Franklin MS, Kraemer GW, Shelton SE, Baker E, Kalin NH, Uno H. Gender differences in brain volume and size of corpus callosum and amygdala of rhesus monkey measured from MRI images. Brain Research. 2000; 852(2):263–267. [PubMed: 10678751]

Frazier TW, Hardan AY. A meta-analysis of the corpus callosum in autism. Biological Psychiatry. 2009; 66(10):935–941. [PubMed: 19748080]

Freitag CM, Luders E, Hulst HE, Narr KL, Thompson PM, Toga AW, Krick C, Konrad C. Total brain volume and corpus callosum size in medication-naïve adolescents and young adults with autism spectrum disorder. Biological Psychiatry. 2009; 66(4):316–319. [PubMed: 19409535]

Giedd JN, Blumenthal J, Jeffries NO, Rajapakse JC, Vaituzis AC, Liu H, Berry YC, Tobin M, Nelson J, Castellanos FX. Development of the human corpus callosum during childhood and adolescence: A longitudinal MRI study. Progress in Neuro-Psychopharmacology and Biological Psychiatry. 1999; 23(4):571–588. [PubMed: 10390717]

Giedd JN, Rumsey JM, Castellanos FX, Rajapakse JC, Kaysen D, Vaituzis AC, Vauss YC, Hamburger SD, Rapoport JL. A quantitative MRI study of the corpus callosum in children and adolescents. Developmental Brain Research. 1996; 91(2):274–280. [PubMed: 8852379]

Glavis-Bloom C, Alvarado M, Bachevalier J. Neonatal hippocampal damage impairs specific food/place associations in adult macaques. Behavioral Neuroscience. 2013; 127:9–22. [PubMed: 23398438]

Gothard K. The amygdalo-motor pathways and the control of facial expressions. Frontiers in Neuroscience. 2014; 8(article 43):1–7. [PubMed: 24478622]

Goursaud AP, Bachevalier J. Social attachment in juvenile monkeys with neonatal lesions of the hippocampus, amygdala and orbital frontal cortex. Behavioural Brain Research. 2007; 176:75–93. [PubMed: 17084912]

Gundersen HJ, Jensen EB. The efficiency of systematic sampling in stereology and its prediction. Journal of Microscopy. 1987; 147(Pt 3):229–263. [PubMed: 3430576]

Haas BW, Barnea-Goraly N, Sheau KE, Yamagata B, Ullas S, Reiss AL. Altered microstructure within social-cognitive brain networks during childhood in Williams syndrome. Cerebral Cortex. 2014; 24(10):2798–2806.

Hadjikhani N, Joseph RM, Snyder J, Tager-Flusberg H. Anatomical differences in the mirror neuron system and social cognition network in autism. Cerebral Cortex. 2006; 16(9):1276–1282. [PubMed: 16306324]

Heuer E, Bachevalier J. Neonatal hippocampal lesions in rhesus macaques alter the monitoring but not maintenance of information in working memory. Behavioral Neuroscience. 2011; 125(6):859–870. [PubMed: 21928873]

Heuer E, Bachevalier J. Working memory for temporal order is impaired after selective neonatal hippocampal lesions in adult rhesus macaques. Behavioural Brain Research. 2013; 239:55–62. [PubMed: 23137699]

Hopkins WD, Phillips KA. Cross-sectional analysis of the association between age and corpus callosum size in chimpanzees (*Pan troglodytes*). Developmental Psychobiology. 2010; 52(2):133–141. [PubMed: 20091760]

Howell BR, McCromack KM, Grand AP, Sawyer NT, Zhang X, Maestripieri D, Hu X, Sánchez MM. Brain white matter microstructure alterations in adolescent rhesus monkeys exposed to early life stress: Associations with high cortisol during infancy. Biology of Mood & Anxiety Disorders. 2013; 3(1):21. [PubMed: 24289263]

Hunsaker MR, Scott JA, Bauman MD, Schumann CM, Amaral DG. Postnatal development of the hippocampus in the rhesus macaque (*Macaca mulatta*): A longitudinal magnetic resonance imaging study. Hippocampus. 2014; 24(7):794–807. [PubMed: 24648155]

Insausti R, Amaral DG. Entorhinal cortex of the monkey: IV Topographical and laminar organization of cortical afferents. Journal of Comparative Neurology. 2008; 509(6):608–641. [PubMed: 18551518]

Just MA, Cherkassky VL, Keller TA, Kana RK, Minshew NJ. Functional and anatomical cortical underconnectivity in autism: Evidence from an FMRI study of an executive function task and corpus callosum morphometry. Cerebral Cortex. 2007; 17(4):951–961. [PubMed: 16772313]

Just MA, Cherkassky VL, Keller TA, Minshew NJ. Cortical activation and synchronization during sentence comprehension in high functioning autism: Evidence of underconnectivity. Brain: A Journal of Neurology. 2004; 127(Pt 8):1811–1821. [PubMed: 15215213]

Kazama AM, Bachevalier J. Preserved stimulus-reward and reversal learning after selective neonatal orbital frontal areas 11/13 or amygdala lesions in monkeys. Developmental Cognitive Neuroscience. 2012; 2(3):363–380. [PubMed: 22494813]

Kazama A, Bachevalier J. Effects of selective neonatal amygdala damage on concurrent discrimination learning and reinforce devaluation in monkeys. Journal of Psychology & Psychotherapy. 2013; Suppl7:5.

Kazama AM, Heuer E, Davis M, Bachevalier J. Effects of neonatal amygdala lesions on fear learning, conditioned inhibition, and extinction in adult macaques. Behavioral Neuroscience. 2012; 126(3):392–403. [PubMed: 22642884]

Knickmeyer RC, Styner M, Short SJ, Lubach GR, Kang C, Hamer R, Coe CL, Gilmore JH. Maturational trajectories of cortical brain development through the pubertal transition: Unique species and sex differences in the monkey revealed through structural magnetic resonance imaging. Cerebral Cortex. 2010; 20(5):1053–1063. [PubMed: 19703936]

Koshino H, Kana RK, Keller TA, Cherkassky VL, Minshew NJ, Just MA. fMRI investigation of working memory for faces in autism: Visual coding and underconnectivity with frontal areas. Cerebral Cortex. 2008; 18(2):289–300. [PubMed: 17517680]

LaMantia AS, Rakic P. Axon overproduction and elimination in the corpus callosum of the developing rhesus monkey. Journal of Neuroscience. 1990a; 10(7):2156–2175. [PubMed: 2376772]

LaMantia AS, Rakic P. Cytological and quantitative characteristics of four cerebral commissures in the rhesus monkey. Journal of Comparative Neurology. 1990b; 291(4):520–537. [PubMed: 2329189]

Lavenex P1, Suzuki WA, Amaral DG. Perirhinal and parahippocampal cortices of the macaque monkey: Projections to the neocortex. Journal of Comparative Neurology. 2002; 447(4):394–420. [PubMed: 11992524]

Lenroot RK, Giedd J. Brain development in children and adolescents: insights from anatomical magnetic resonance imaging. Neuroscience & Biobehavioral Reviews. 2006; 30(6):718–729. [PubMed: 16887188]

Levy J, Trevarthen C. Color-matching, color naming and color memory in split brain patients. Neuropsychologia. 1981; 19(4):523–541. [PubMed: 7279185]

Luders E, De Paola M, Tomaiuolo F, Thompson PM, Toga AQ, Vicari S, Petreides M, Caltagirone C. Callosal morphology in Williams syndrome: A new evaluation of shape and thickness. NeuroReport. 2007; 18(3):203–207. [PubMed: 17314657]

Luders E, Thompson PM, Toga AW. The development of the corpus callosum in the healthy human brain. Journal of Neuroscience. 2010; 30(33):10985–10990. [PubMed: 20720105]

Machado CJ, Bachevalier J. Non-human primate models of childhood psychopathology: the promise and the limitations. The Journal of Child Psychology and Psychiatry. 2003; 44(1):64–87. [PubMed: 12553413]

Meda SA, Pryweller JR, Thornton-Wells TA. Regional brain differences in cortical thickness, surface area and subcortical volume in individuals with Williams syndrome. PLoS One. 2012; 7(2):e31913. [PubMed: 22355403]

Morecraft RJ, McNeal DW, Stilwell-Morecraft KS, Gedney M, Ge J, Schroeder CM, Van Hoesen GW. Amygdala interconnections with the cingulate motor cortex in the rhesus monkey. Journal of Comparative Neurology. 2007; 500(1):134–165. [PubMed: 17099887]

Paus T. Primate anterior cingulate cortex: Where motor control, drive and cognition interface. Nature Reviews Neuroscience. 2001; 2:417–424. [PubMed: 11389475]

Payne C, Machado CJ, Bliwise NG, Bachevalier J. Maturation of the hippocampal formation and amygdala in *Macaca mulatta*: A volumetric magnetic resonance imaging study. Hippocampus. 2010; 20(8):922–935. [PubMed: 19739247]

Payne, C., Machado, CJ., Jackson, EF., Bachevalier, J. Neuroscience Meeting Planner. Washington, DC: Society for Neuroscience Online; 2005. Maturation of the rhesus monkey primate corpus callosum: A structural MRI study. Program No. 195.9

Phillips KA, Kochunov P. Tracking development of the corpus callosum in fetal and early postnatal baboons using magnetic resonance imaging. The Open Neuroimaging Journal. 2011; 5:179–185. [PubMed: 22253660]

Phillips KA, Sherwood CC. Age-related differences in corpus callosum of capuchin monkeys. Neuroscience. 2012; 202:202–208. [PubMed: 22173013]

Pierre PJ, Hopkins WD, Taglialatela JP, Lees CJ, Bennett AJ. Age-related neuroanatomical differences from the juvenile period to adulthood in mother-reared macaques (*Macaca radiata*). Brain Research. 2008; 1226:56–60. [PubMed: 18619575]

Rakic P, Yakovlev PI. Development of the corpus callosum and cavum septi in man. Journal of Comparative Neurology. 1968; 132(1):45–72. [PubMed: 5293999]

Raper J, Wilson ME, Sánchez MM, Bachevalier J. Neonatal amygdala lesions alter emotional and neuroendocrine responses to an acute stressor in adult rhesus monkeys. Paper presented at the Gordon Research Conference: Amygdala in Health and Disease. 2011

Raymond GV, Bauman ML, Kemper TL. Hippocampus in autism: A golgi analysis. Acta Neuropathologica. 1996; 91:117–119. [PubMed: 8773156]

Rommeck I, Capitanio JP, Strand SC, McCowan B. Early social experience affects behavioral and physiological responsiveness to stressful conditions in infant rhesus macaques (*Macaca mulatta*). American Journal of Primatology. 2011; 73(7):692–701. [PubMed: 21462233]

Rosene DL, Van Hoesen GW. Hippocampal efferents reach widespread areas of cerebral cortex and amygdala in the rhesus monkey. Science. 1977; 198:315–317. [PubMed: 410102]

Rosselli M, Ardila A, Maute E, Inozemtseva O. Gender differences and cognitive correlates of mathematical skills in school-aged children. Child Neuropsychology: A Journal on Normal and Abnormal Development in Childhood and Adolescence. 2009; 15(3):216–231. [PubMed: 18608220]

Saitoh O, Karns CM, Courchesne E. Development of the hippocampal formation from 2–42 years-MRI evidence of smaller area dentata in autism. Brain: A Journal of Neurology. 2001; 124(Pt7): 1317–1324. [PubMed: 11408327]

Sampaio A, Sousa N, Férnandez M, Henriques M, Gonçalves OF. Memory abilities in Williams syndrome: Dissociation or developmental delay hypothesis? Brain and Cognition. 2008; 66(3): 290–297. [PubMed: 17950967]

Sánchez MM, Hearn EF, Do D, Rilling JK, Herndon JG. Differential rearing affects corpus callosum size and cognitive function of rhesus monkeys. Brain Research. 1998; 812(1–2):38–49. [PubMed: 9813233]

Schlaug G, Jancke L, Huang Y, Staiger JF, Steinmetz H. Increased corpus callosum size in musicians. Neuropsychologia. 1995; 33(8):1047–1055. [PubMed: 8524453]

Schmahmann, JD., Pandya, DN. Corpus callosum. In: Schmahmann, JD., Pandya, DN., editors. Fiber pathways of the brain. New York, NY: Oxford UP; 2006. p. 485-496.

Shanks MF, Rockel AJ, Powel TPS. The commissural fiber connections of the primary somatic sensory cortex. Brain Research. 1975; 98(1):166–171. [PubMed: 809118]

Shi Y, Short SJ, Knickmeyer RC, Wang J, Coe CL, Niethammer M, Gilmore JH, Zhu H, Styner M. Diffusion tensor imaging-based characterization of brain development in primates. Cerebral Cortex. 2013; 23(1):36–48. [PubMed: 22275483]

Takeuchi H, Sekiguchi A, Taki Y, Yokoyama S, Yomogida Y, Komuro N, Yamanouchi T, Suzuki S, Kawashima R. Training of working memory impacts structural connectivity. Journal of Neuroscience. 2010; 30:3297–3303. [PubMed: 20203189]

Travers BG, Adiuru N, Ennis C, Tromp do PM, Destiche D, Doran S, Bigler ED, Lange N, Lainhart JE, Alexander AL. Diffusion tensor imaging in autism spectrum disorder: A review. Autism Research. 2012; 5(5):289–313. [PubMed: 22786754]

Ungerleider LG, Gaffan D, Pelak VS. Projections from inferior temporal cortex to prefrontal cortex via the uncinate fascicle in rhesus monkeys. Experimental Brain Research. 1989; 76:473–484. [PubMed: 2792241]

Unterrainer JM, Ruth N, Loosli SV, Heinze K, Rahm B, Kaller CP. Planning steps forward in development: In girls earlier than in boys. PLoS One. 2013; 8(11):e80772. [PubMed: 24312240]

Vicari S, Brizzolara D, Carlesimo GA, Pezzini G, Volterra V. Memory abilities in children with Williams syndrome. Cortex. 1996; 32(3):503–514. [PubMed: 8886525]

Volkmar FR, Lord C, Bailey A, Schultz RT, Klin A. Autism and pervasive developmental disorders. The Journal of Child Psychology and Psychiatry. 2004; 45(1):135–170. [PubMed: 14959806]

Wade BSC, Stockman M, McLaughlin MJ, Raznahan A, Lalonde F, Giedd JN. Improved corpus callosum area measurements by analysis of adjoining parasagittal slices. Psychiatry Research: Neuroimaging. 2013; 211(3):221–225. [PubMed: 23149042]

Waiter GD, Williams JH, Murray AD, Gilchrist A, Perrett DI, Whiten A. Structural white matter deficits in high-functioning individuals with autistic spectrum disorder: A voxel-based investigation. NeuroImage. 2005; 24(2):455–461. [PubMed: 15627587]

Witelson SF. Hand and sex differences in the isthmus and genu of the human corpus callosum: A postmortem morphological study. Brain: A Journal of Neurology. 1989; 112(Pt 3):799–835. [PubMed: 2731030]

Zahr NM, Rohlfing T, Pfefferabaum A, Sullivan EV. Problem solving, working memory, and motor correlates of association and commissural fiber bundles in normal aging: A quantitative fiber tracking study. NeuroImage. 2009; 44(3):1050–1062. [PubMed: 18977450]

Zaidel D, Sperry RW. Memory impairment after commisurotomy in man. Brain: A Journal of Neurology. 1974; 97(2):263–272. [PubMed: 4434177]

Zaidel D, Sperry RW. Some long-term motor effects of cerebral commissurotomy in man. Neuropsychologia. 1977; 15(2):193–204. [PubMed: 846629]

Zeamer A, Bachevalier J. Long-term effects of neonatal hippocampal lesions on novelty preference in monkeys. Hippocampus. 2013; 23(9):745–750. [PubMed: 23640834]

Zeamer A, Heuer E, Bachevalier J. Developmental trajectory of object recognition memory in infant rhesus macaques with and without neonatal hippocampal lesions. Journal of Neuroscience. 2010; 30(27):9157–9165. [PubMed: 20610749]

Zeamer, AE., Kazama, AM., Briseno, B., Bachevalier, J. Program No 791.3 Neuroscience Meeting Planner. Washington, DC: Society for Neuroscience Online; 2008. Intact object recognition memory after damage to orbital frontal areas 11 and 13 in adult macaque monkeys.

Zeamer, AE., Resende, M., Heuer, E., Bachevalier, J. Program No 195.8 Neuroscience Meeting Planner. San Diego, CA: Society for Neuroscience Online; 2007. The development of infant monkeys' recognition memory abilities in the absence of a functional hippocampus.
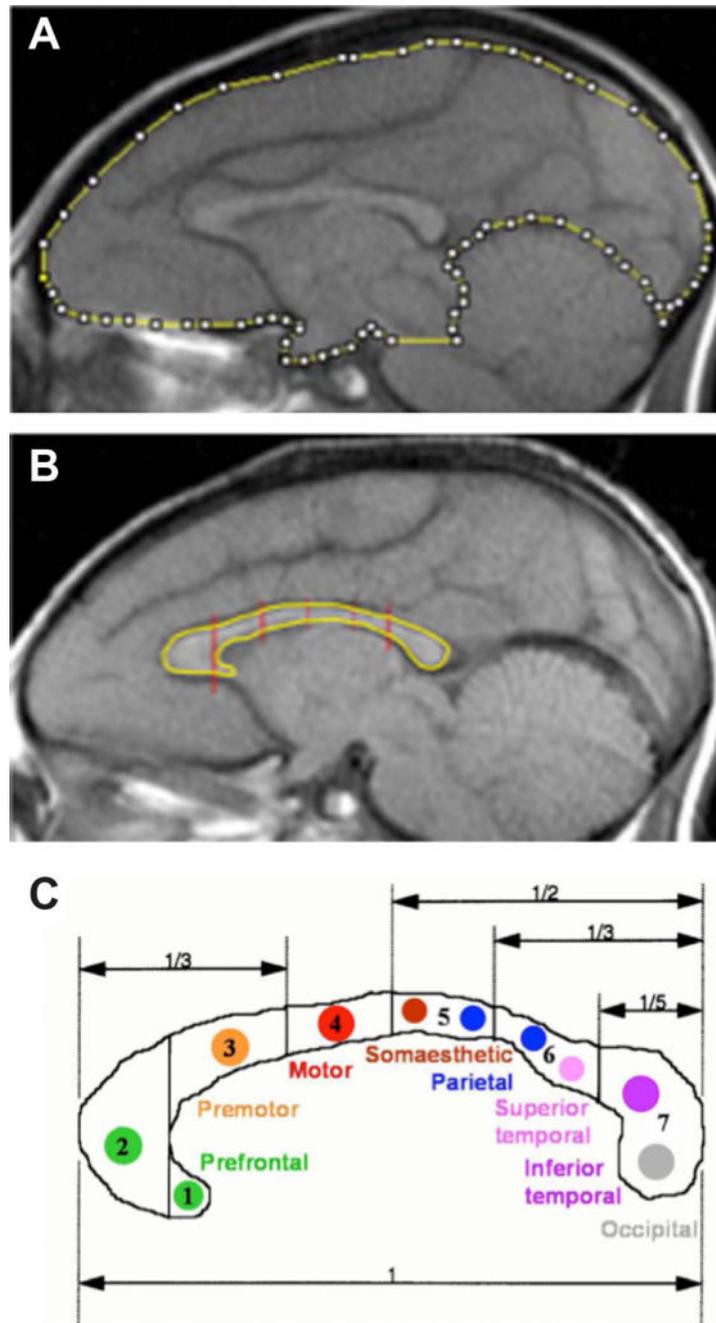
Figure 1. CC Borders and Segmentation
Sample sagittal MR images with the measurements for (A) the midline brain SA and (B) the CC with its segmentation. (C) Regional and functional subdivisions of the CC from (Witelson, 1989). Subsections: (1) rostrum, (2) genu, (3) rostral body, (4) anterior midbody, (5) posterior midbody, (6) isthmus and (7) splenium.
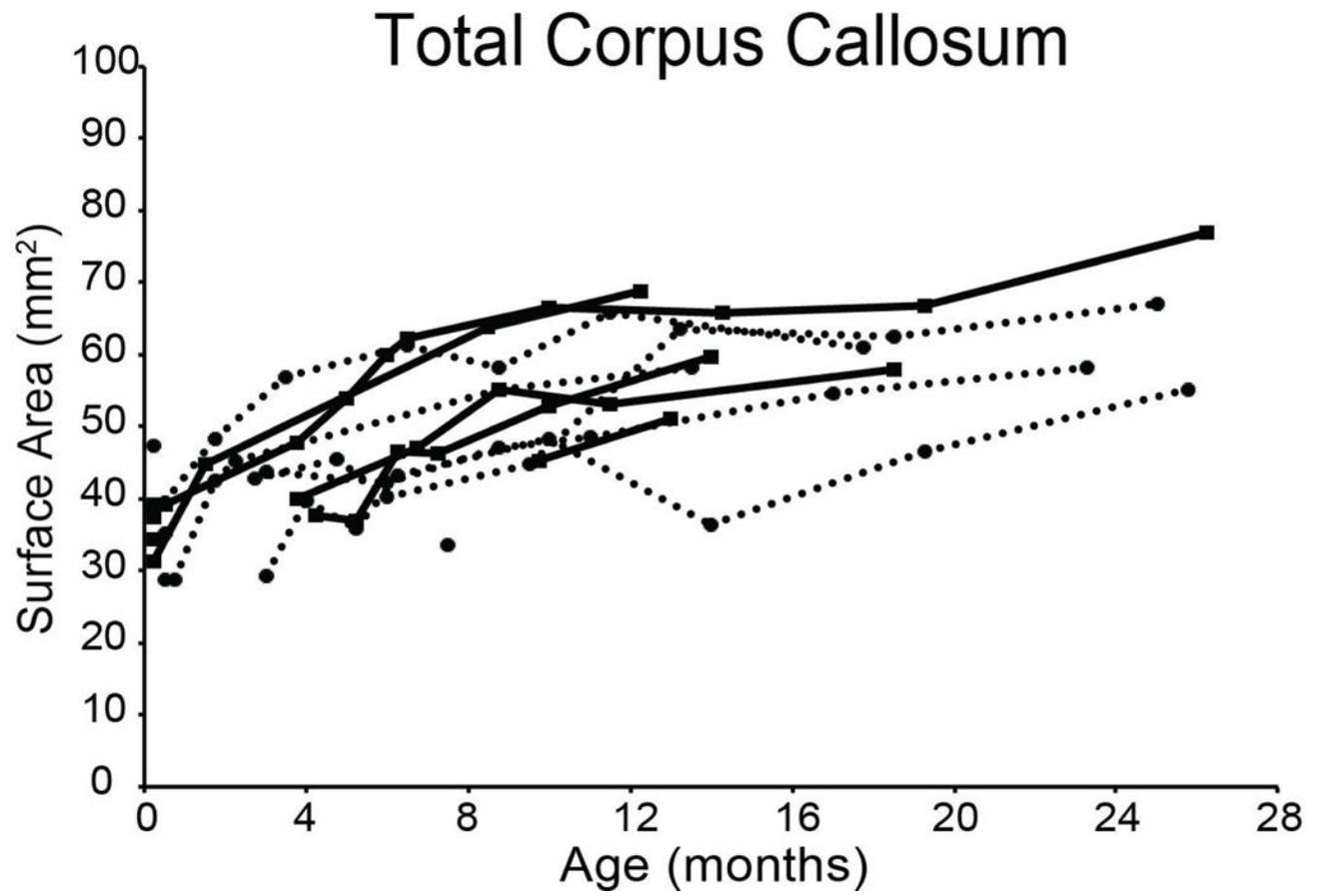
Figure 2. CC Surface Area as a Function of Age
Scatterplot of raw surface areal measurements for the CC as a whole in squared millimeters
as a function of age in months. Filled squares denote males and filled circles denote females.
Lines between data points represent longitudinal measurements on the same animal for
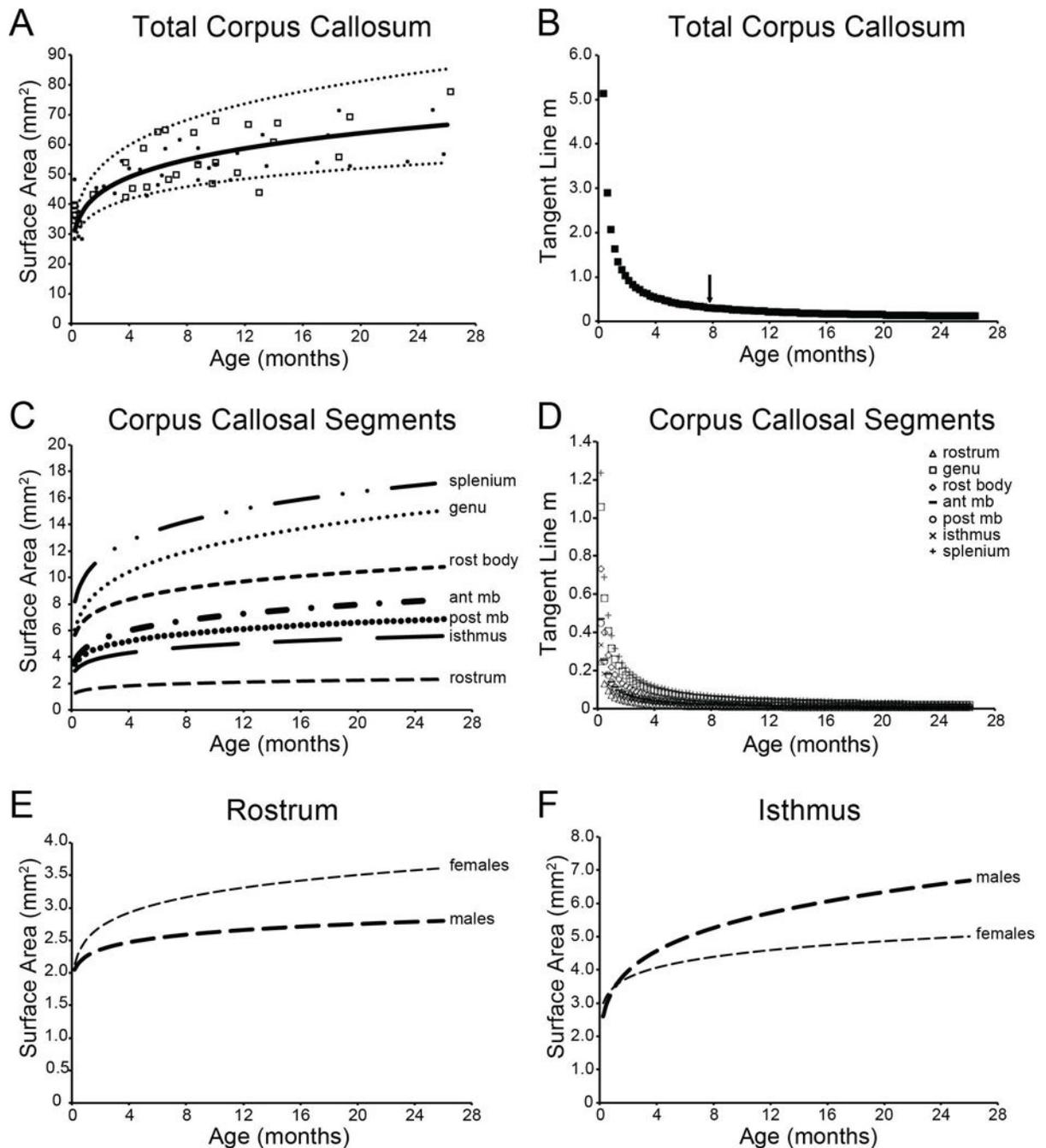males (solid) and females (dashed).

Figure 3. Modeled Trajectories and Growth Rates

Top panels represent the modeled developmental trajectory (A) and tangent line slope values (B) for the modeled function for the total CC surface area. Individual surface areas are represented by open squares (males) and open circles (females). Arrow indicates the age at which differences between two adjacent data points did not substantially differ, and thus represents the approximate age at which growth leveled off. Middle panels represent the modeled developmental trajectory (C) and tangent line slope (m) values (D) for the modeled function for the individual callosal segments. Bottom panels represent the developmental

trajectories modeled separately for males and females for the rostrum (E) and isthmus (F). All modeled trajectories include MSA to account for differences in overall brain size. rost body = rostral body; ant mb = anterior midbody; post mb = posterior midbody

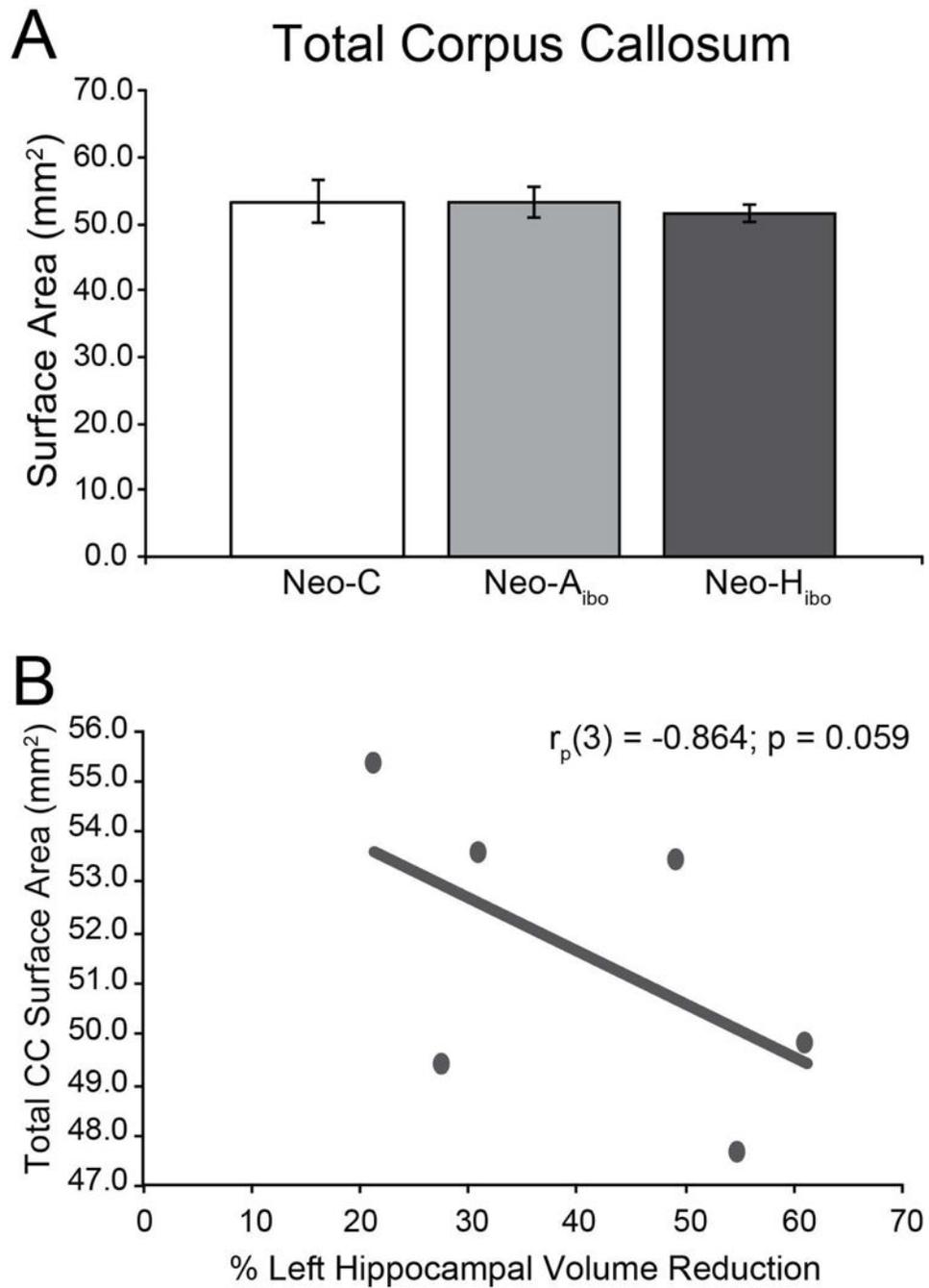**Figure 4. Effect of Lesions on Total CC**
Average surface area of total CC (in mm^2) for (A) group CONT (white bar), group NEO-A$_{ibo}$ (light grey bar) and group NEO-H$_{ibo}$ (dark grey bar). Error bars denote standard error of the mean (SEM); no significant group differences were observed. Partial correlation between total CC surface area and the extent of intended damage for group NEO-H$_{ibo}$ (B).

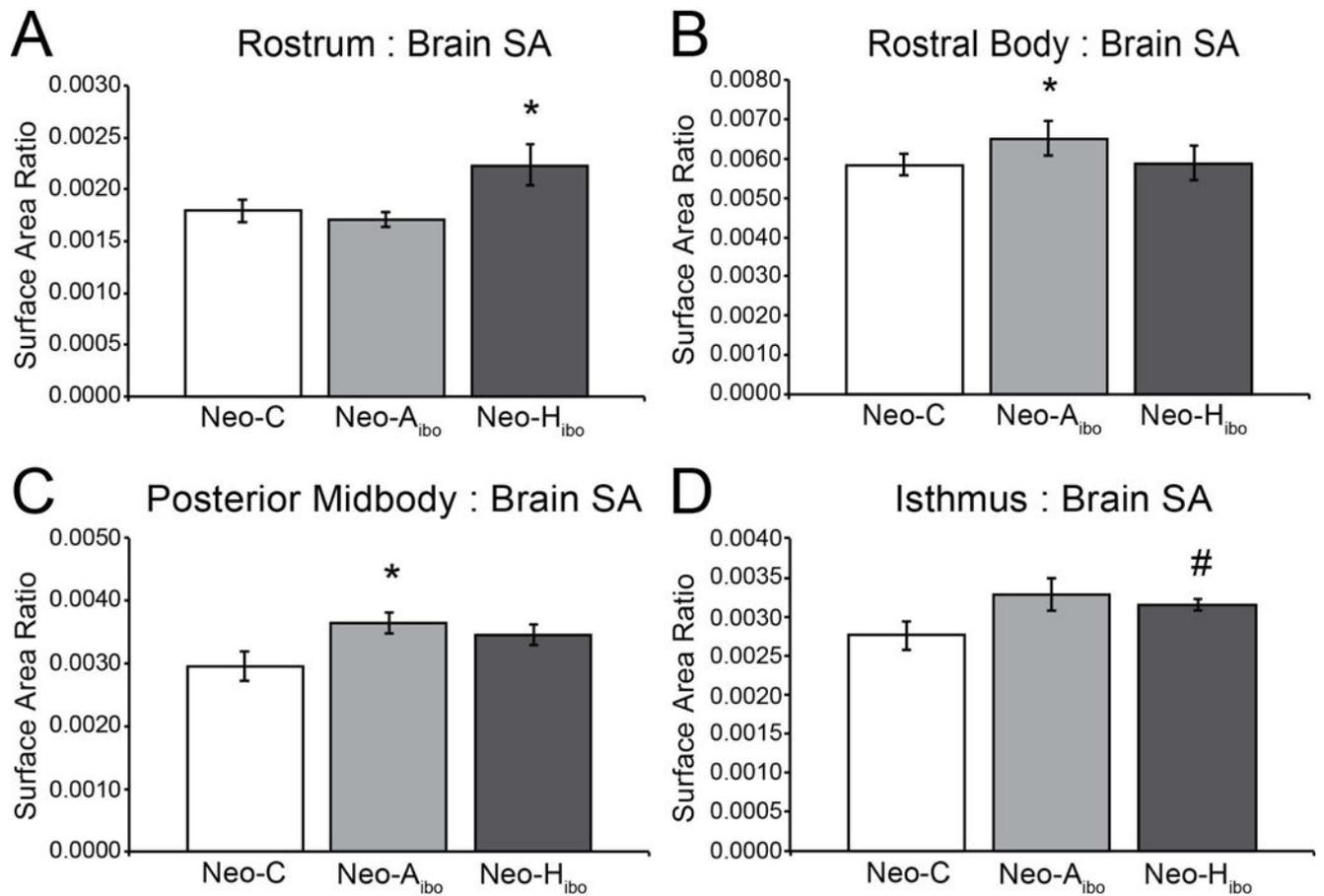**Figure 5. Surface Area of Segments by Group**
Average surface areas represented as a ratio between segment surface area and midsagittal surface are for group CONT (white bar), group NEO-A$_{ibo}$ (light grey bar) and group NEO-H$_{ibo}$ (dark grey bar) of the rostrum (A), rostral body (B), posterior midbody (D) and isthmus (E). Error bars denote standard error of the mean (SEM). *: $p < 0.05$; #: $p < 0.08$.

Table 1

Percent Volume Reduction Following Neonatal Lesion Relative to Age- and Sex-Matched Control Group.

		Amygdala		
Case	Sex	L	R	$\overline{X}$
NEO-A_{ibo}-1	F	41.5	43.7	42.6
NEO-A_{ibo}-2	M	14.4	35.2	25.3
NEO-A_{ibo}-3	F	14.7	24.1	19.6
NEO-A_{ibo}-4	M	38.5	41.1	39.9
NEO-A_{ibo}-5	F	19.7	37.8	29.2
NEO-A_{ibo}-6	M	19.8	38.4	29.6
	Mean	24.8	36.7	31.0

		Hippocampus		
Cases	Sex	L	R	$\overline{X}$
NEO-H_{ibo}-1	M	27.6	10.8	19.1
NEO-H_{ibo}-2	M	61.2	72.8	67.0
NEO-H_{ibo}-3	F	54.7	47.8	51.3
NEO-H_{ibo}-4	M	31.1	59.2	45.1
NEO-H_{ibo}-5	F	49.2	64.0	56.6
NEO-H_{ibo}-6	M	21.3	8.3	14.8
	Mean	40.8	43.8	42.3

L: percent volume reduction in the left hemisphere;

R: percent volume reduction in the right hemisphere;

$\overline{X}$: average percent volume reduction in both hemispheres.

Table 2

CC Surface Area Measurements by Group.

Group	Midline	Total CC	Rostrum	Genu	Rostral Body	Anterior Midbody	Posterior Midbody	Isthmus	Splenium
CONT	**1532.9**	**53.3**	**2.8**	**14.5**	**9.0**	**5.9**	**4.6**	**4.2**	**12.3**
	(± 39.2)	**(3.2)**	**(0.2)**	**(1.5)**	**(0.6)**	**(0.4)**	**(0.4)**	**(0.4)**	**(0.7)**
Males	1501.5	54.2	2.8	14.3	9.2	5.9	4.8	4.4	12.9
	(± 56.0)	(5.6)	(0.4)	(2.7)	(0.7)	(0.5)	(0.2)	(0.5)	(1.0)
Females	1555.2	52.5	2.7	14.8	8.8	6.0	4.3	4.1	11.8
	(± 63.7)	(4.2)	(0.1)	(2.1)	(1.1)	(0.8)	(0.9)	(0.5)	(0.9)
NEO-A$_{ibo}$	**1480.2**	**53.4**	**2.5**	**12.4**	**9.7** *α	**5.7**	**5.4** *α	**4.9** α	**12.8**
	(± 42.2)	**(2.4)**	**(0.1)**	**(1.1)**	**(0.8)**	**(0.6)**	**(0.3)**	**(0.4)**	**(0.6)**
Males	1451.2	50.2	2.6	10.4	10.5	4.7	4.8	4.3	12.8
	(± 70.2)	(1.7)	(0.2)	(1.2)	(1.5)	(0.5)	(0.01)	(0.1)	(0.8)
Females	1509.3	56.6	2.4	14.4	8.9	6.7	6.0	5.4	12.8
	(± 56.0)	(3.9)	(0.2)	(1.0)	(0.6)	(0.8)	(0.4)	(0.6)	(1.0)
NEO-H$_{ibo}$	**1421.1**	**51.6** α	**3.2** *α	**12.3**	**8.3** α	**5.6**	**4.9**	**4.5** †	**12.8**
	(± 29.8)	**(1.2)**	**(0.3)**	**(0.8)**	**(0.6)**	**(0.5)**	**(0.2)**	**(0.1)**	**(0.3)**
Males	1437.4	52.1	3.5	12.5	8.7	5.1	6.0	4.6	12.7
	(± 43.9)	(1.4)	(0.4)	(1.3)	(0.8)	(0.1)	(0.4)	(0.2)	(0.4)
Females	1388.5	50.5	2.6	11.7	7.5	6.7	4.9	4.3	12.8
	(± 14.1)	(2.9)	(0.1)	(0.01)	(0.3)	(1.3)	(0.2)	(0.3)	(0.9)

Average surface area measurements in mm^2 (± sem; in parentheses) for each group as a whole (bold) as well as separately for males and females.

†
denotes trend for Group effect (compared to group CONT);

*
denotes significant Group effect; α denotes negative correlation with structure volume.